Chapter 3

Analytical Modeling of Subthreshold Current and Subthreshold Swing of DG-JLFETs with a Vertical Gaussian-Like Channel Profile

3.1 Introduction

We have already discussed in Chapter-1 that the subthreshold current and subthreshold swing (SS) are very important performance parameters of the MOS transistors. While the subthreshold current determines the static power loss of the device in analog/digital ICs applications, the SS determines the switching characteristics of the transistors for digital circuits and systems applications. Based on the TCAD simulation results, Mondal *et al.* [Mondal *et al.*(2013), Mondal *et al.*(2015)] have shown that the profile parameters of a vertical Gaussian doping in the channel can be used for optimizing the OFF-state current of the JL SOI-FETs [Mondal *et al.*(2013)] and JL-FinFETs [Mondal *et al.*(2015)]. Thus, after investigating the potential distribution and threshold voltage characteristics in Chapter-2 of the DG JLFETs with a vertical Gaussian-like non-uniform channel profile, we are now interested in developing the analytical models for the subthreshold current and subthreshold swing of the device in the present chapter. All definitions of the device and doping profile parameters considered in Chapter-2 will be also used in this chapter. Some of the results/expressions developed in Chapter-2 will

also be directly used in this chapter. The layout of the present chapter can be given as follows:

In Sec.3.2, we have used the channel potential model derived in Sec.2.2 for the modeling of subthreshold current and subthreshold swing of the DG-JLFETs. For validating our proposed models, the model results have been compared with the ATLAS^{TM} TCAD simulation data for different gate lengths, straggle parameter values, oxide thicknesses, channel thicknesses, and peak doping concentrations of the device. Section 3.4 has been used for the summary and conclusion of the present chapter.

3.2 Model Derivation

The cross-sectional view of DG-JLFET structure considered for the present study is shown in Fig.3.1. Although, the device structure used in this chapter is same as considered in Chapter 2 (Fig. 2.1), it is reproduced here for the better understanding of the work carried out in this chapter. The gate oxide thickness, channel length, and channel thickness are denoted by t_{ox}, L, and t_{si}, respectively. Both the gates are connected with common gate-to-source voltage (V_{gs}) and the drain is connected with Drain-to-source voltage (V_{ds}). The x and y-axes are considered along with the channel thickness and along channel length from source to drain respectively.

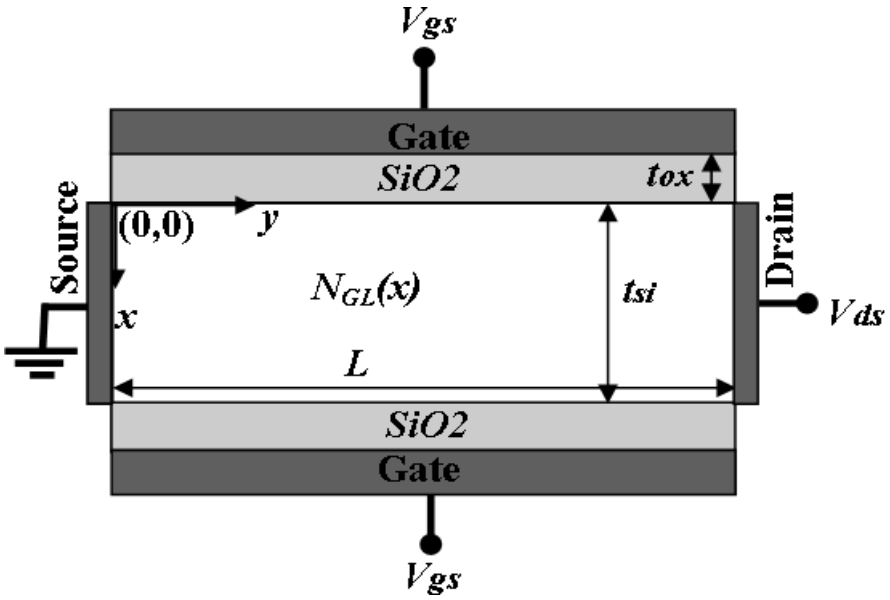

Fig. 3.1: Simplified two-dimensional cross-sectional view of DG- JLFET.

The Gaussian-like doping profile, say $N_{GL}(x) \approx N(x)$ is assumed to be same as in chapter 2, is reproduced here as

$$N_{GL}(x) = cN_{pk}\left((a+2b\alpha X)^2 - 2b\right)\exp(-a\alpha X - bX^2) \tag{3.1}$$

where, $a = 1.786, b = 0.646$ and $c = 0.56$ are fitting parameters; $\alpha = +1$ for $x > 0$ and $\alpha = -1 \text{ for } x < 0$; $X = \dfrac{x - R_p}{\sqrt{2}\sigma_p}$ where R_p is the projected range and σ_p is the straggle of the Gaussian doping profile; and $N_{pk} = Q \Big/ \sqrt{2\pi\sigma_p^2}$ is the peak doping at $x = R_p$.Since the present model is the continuation of the previous work presented in Chapter 2, all device parameters in the present model are used with the same terminology as in Chapter 2. Also, some of the results of Chapter 2 have been

considered directly for developing the subthreshold current and SS models of the device as follows:

3.2.1 Subthreshold Current Model

The subthreshold current using the analytical channel potential can be written as [Jin *et al.(2012),*Lin *et al.*(2012)].

$$I_{DS} = \frac{q\mu_n W V_T n_{ieff}\left(1-\exp\left(-\frac{V_{ds}}{V_T}\right)\right)}{\int_0^L \frac{dy}{\int_0^{t_{si}} \exp\left(\frac{\psi(x,y)}{V_T}\right)dx}} \tag{3.2}$$

where μ_n, W, V_T, n_{ieff}, L and $\psi(x,y)$ are the effective electron mobility, channel width, thermal voltage, effective intrinsic concentration, channel length and 2D potential function derived in chapter 2, respectively.

It is important to note that the subthreshold current is limited by the charge carrier density at the minimum channel potential along the transport direction [Lin et *al.*(2012)] Thus, the expression for the subthreshold current can be written as:

$$I_{DS} = \frac{q\mu_n W V_T n_{ieff}\left(1-\exp\left(-\frac{V_{ds}}{V_T}\right)\right)}{\int_0^L \frac{dy}{\int_0^{t_{si}} \exp\left(\frac{\psi(x,y)\big|_{y=y_{\min}}}{V_T}\right)dx}} \tag{3.3}$$

From the Chapter 2, the minimum channel potential is given as:

$$\psi_{\min}(x) = \psi(x,y)\big|_{y=y_{\min}} = U(x) + V(x, y_{\min}) \tag{3.4}$$

which can be re-written as

$$\psi_{\min}(x) = \left[-\frac{q{x_b}^2}{\varepsilon_{si}} \left[cN_{pk} \exp\left(-a\alpha X - bX^2\right) + AX + B \right] + 2\cos(\eta x)\sqrt{V_1 V_1'} \exp\left(-\frac{\eta L}{2}\right) \right] \tag{3.5}$$

After simplification, Eq. (3.5) can be written as

$$\psi(x,y)\big|_{y=y_{\min}} = -I_1 x^2 + I_2 x - I_3 \tag{3.6}$$

where, $I_1 = \left[{x_b}^{-2} McN_{pk} \left(\frac{a^2\alpha^2}{2} - b \right) + \left(\eta^2 \sqrt{V_1 V_1'} \exp\left(-\frac{\eta L}{2}\right) \right) \right]$ (3.7)

$$I_2 = \left[\frac{Ma\alpha N_{pk} c - AM}{x_b} + \frac{2R_p}{{x_b}^2} \left(McN_{pk} \left(\frac{a^2\alpha^2}{2} - b \right) \right) \right] \tag{3.8}$$

$$I_3 = \left[\frac{McN_{pk} {R_p}^2}{{x_b}^2} \left(\frac{a^2\alpha^2}{2} - b \right) + \frac{R_p}{x_b} \left(Ma\alpha N_{pk} c - AM \right) + \left(McN_{pk} + BM \right) - 2\sqrt{V_1 V_1'} \exp\left(-\frac{\eta L}{2}\right) \right] \tag{3.9}$$

Using Eqs.(3.4)-(3.9) in Eq.(3.3), the subthreshold drain current expression can be written as:

$$I_{DS} = \left[K_{Ids} \sqrt{\left(\frac{\pi V_T}{4I_1}\right)} \exp\left(\frac{I_2^2 - 4I_1 I_3}{4I_1 V_T} \right) \times \left\{ erf\left(\frac{2I_1 t_{si} - I_2}{2\sqrt{I_1 V_T}} \right) - erf\left(\frac{-I_2}{2\sqrt{I_1 V_T}} \right) \right\} \right] \tag{3.10}$$

3.2.2 Modeling of Subthreshold Swing

SS is an important parameter to assess the subthreshold switching characteristics of a nanoscale MOS transistor. Mathematically, the SS can be defined as:

$$SS = \left(\frac{\partial \log I_S}{\partial V_{GS}} \right)^{-1} \tag{3.11}$$

The subthreshold current mainly flows through the conduction path (x_C) with minimum conduction path potential $\psi_{\min}(x_C)$ as discussed in Chapter 2. Thus, we consider that the subthreshold current (I_{DS}) is proportional to $\exp\left(\frac{\psi_{\min}(x_C)}{V_T} \right)$. Thus, SS can be expressed as [Hu *et al.*(2014)]

$$SS = \frac{V_T \ln(10)}{\left(\frac{\partial \psi_{\min}(x_C)}{\partial V_{gs}} \right)} \tag{3.12}$$

$$SS = \frac{V_T \ln(10)}{1 + \frac{K_S (V_1 + V_1') Cos(\eta x_C)}{2\sqrt{V_1 V_1'} Sinh(\eta L)} \exp\left(\frac{\eta L}{2} \right)} \tag{3.13}$$

where

$$K_S = -\left(\frac{4Sin(\eta t_{si})}{\eta \left(2t_{si} + \eta^{-1} Sin(2\eta t_{si}) \right)} \right) \tag{3.14}$$

3.3 Results and discussion

In this section, we will present some results related to subthreshold current and SS of the ion-implanted DG- JLFET considered in this chapter. For validation of our proposed model results, we will compare them with their corresponding ATLAS^{TM} based 2D device simulation data. For TCAD simulation, the actual Gaussian doping profile with the same peak doping N_{pk} and straggle parameter (σ_p) are used as in the analytical model. The values of different parameters used for simulation and computations are work function of the gate electrode material $= 5.1\,eV$, $t_{si} = 10nm$, $t_{ox} = 1.5nm$ and $N_{pk} = 1\times10^{19}cm^{-3}$.

The details of the models used for the 2D numerical simulations are same as discussed in Chapter 2. The variations of subthreshold current with gate-to-source voltage for different channel lengths have been plotted in Fig.3.2. The subthreshold current is observed to be increased with the decreased channel length which can be attributed to the loss of gate control over the channel due to the inverse relation of the minimum conduction path potential with the channel length. The deviation of our analytical results from TCAD simulation results is observed beyond certain gate voltage, when the DG-JLFET starts to enter into the ON-state for which our proposed model is not applicable [Jiang *et al.* (2015)].

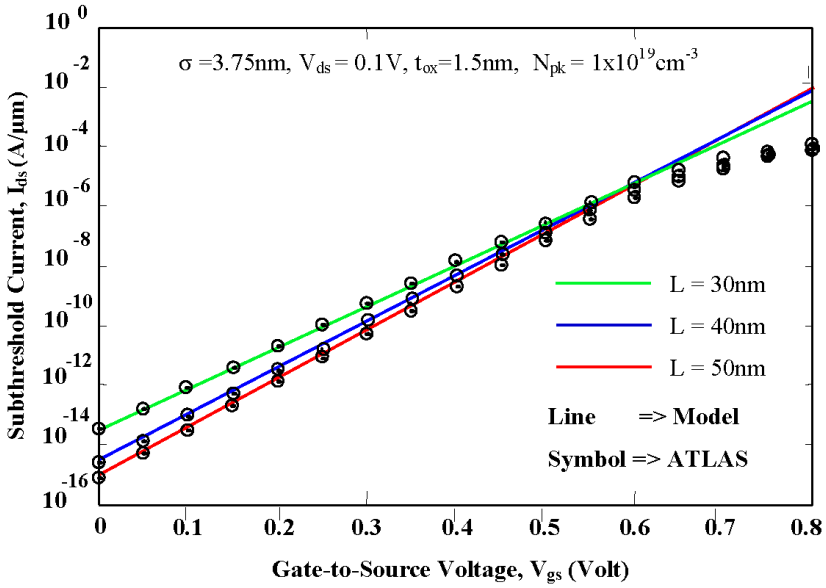

Fig. 3.2: Subthreshold current variation with gate-to-source voltage for different gate lengths.

To investigate the effect of the straggle parameter on the subthreshold drain current, the $I_{ds} - V_{gs}$ characteristics of the vertical Gaussian doped channel DG-JLFET have been plotted in Fig.3.3. The increase in the subthreshold current considerably with the straggle parameter may be due to the increase in the average doping concentration across the channel region.

The effect of gate oxide thickness on the subthreshold current for fixed gate-to-source voltage has been demonstrated in Fig.3.4. The subthreshold current is observed to be increased with the increase in the gate oxide thickness due to the decrease in the gate control over the channel.

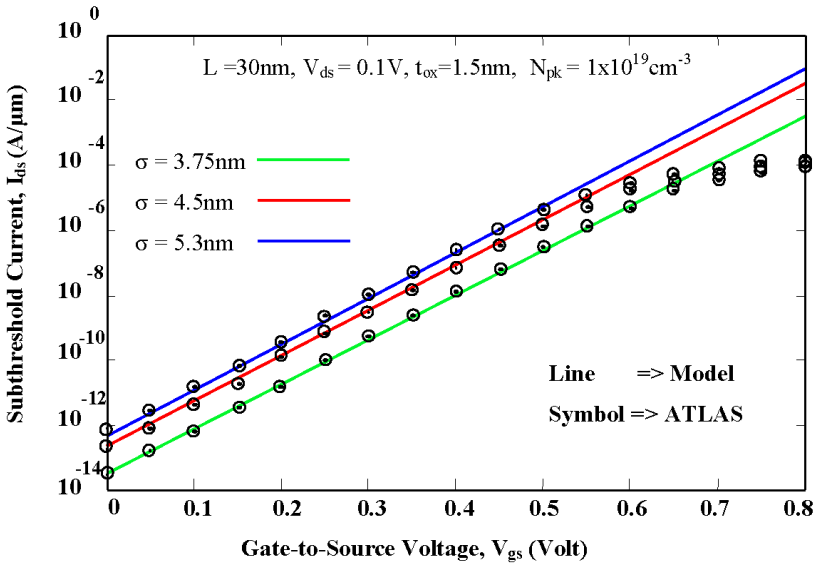

Fig. 3.3: Subthreshold current variation with gate-to-source voltage for different straggle parameter.

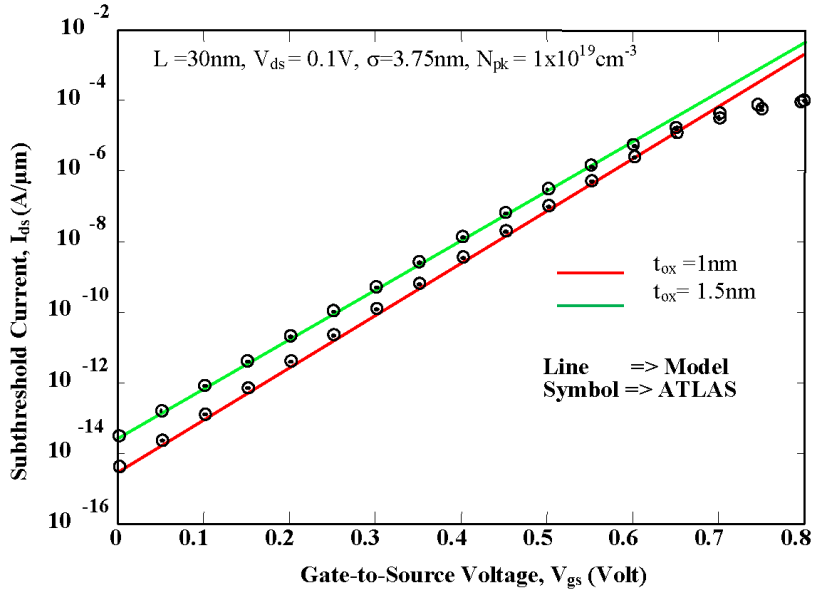

Fig. 3.4: Subthreshold current versus gate-to-source voltage for different oxide thickness.

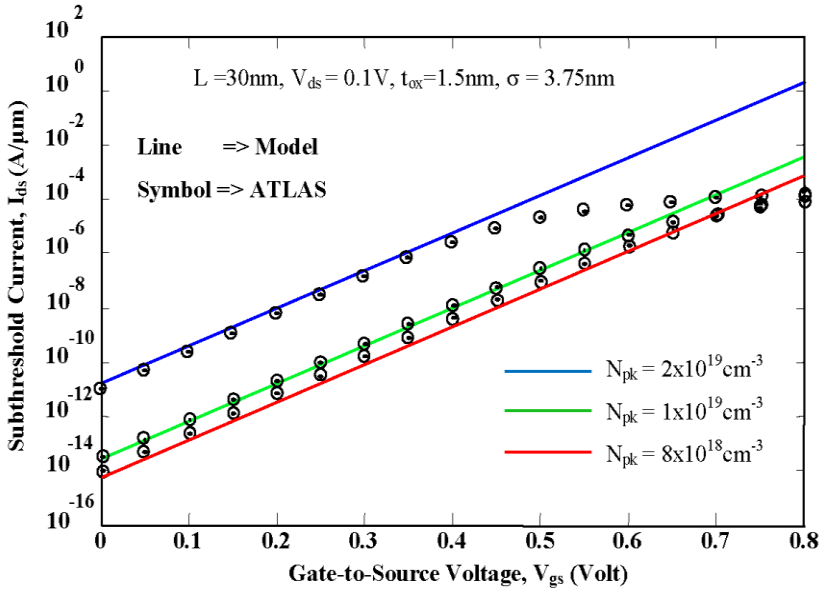

Fig. 3.5: Subthreshold current versus gate-to-source voltage for different peak doping concentration.

In general, the channel of JLFET is desired to be fully depleted in OFF-state condition. The fully depleted channel is converted to the partially depleted channel by applying a suitable gate-bias to achieve the ON-state of the device. The increased channel doping reduces the possibility of being fully depleted unless the channel thickness is reduced. However, reduced channel thickness $t_{Si} < 7\,nm$ may affect the OFF-state gate leakage current due to quantum mechanical effects [Parihar *et al.* (2013)]. Further, the threshold voltage, drive current, leakage current and drain-induced barrier lowering may be severely affected by the random dopant fluctuation for increased doping concentration beyond $1\times10^{19}\ \mathrm{cm}^{-3}$[Leung *et al.* (2012)]. Thus, the analytical model given in this chapter has been validated with TCAD results in Fig.3.5 for peak Gaussian doping concentrations of $8\times10^{18}\ \mathrm{cm}^{-3}$, $1\times10^{19}\ \mathrm{cm}^{-3}$ and $2\times10^{19}\ \mathrm{cm}^{-3}$ to ensure the fully

depleted condition of the channel in the OFF-state operation of the device.

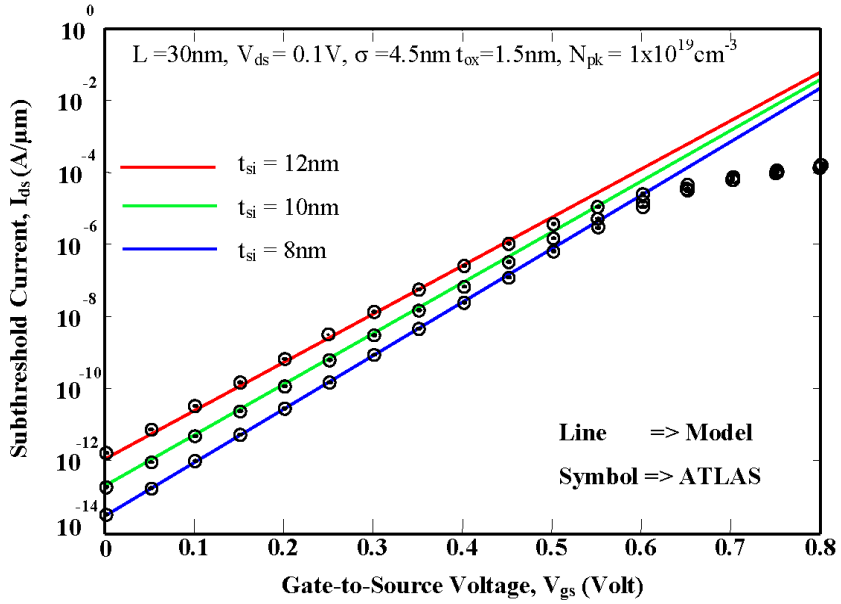

Fig.3.6. Subthreshold current versus gate-to-source voltage for different channel thickness.

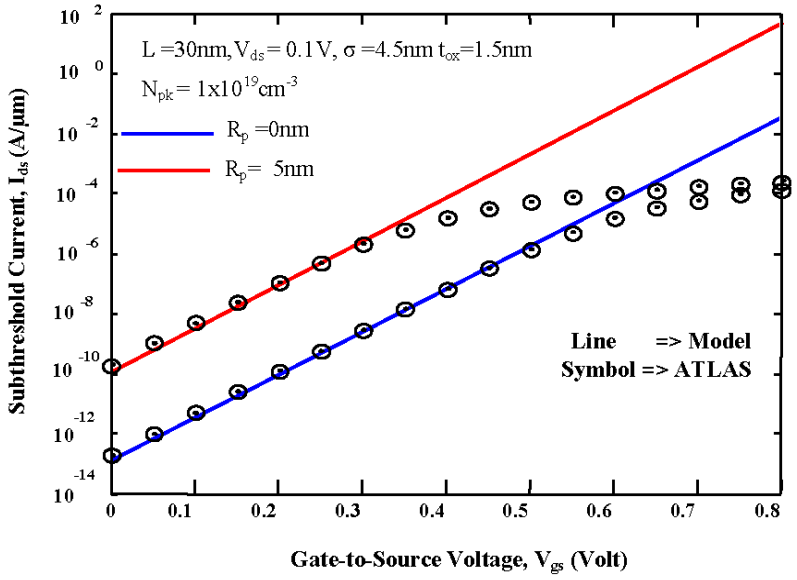

Fig.3.7. Subthreshold current versus gate-to-source voltage for different projected range (R_p).

The increase in the subthreshold current with the peak doping concentration (N_{pk}) is attributed to decrease in the source to channel barrier height with increased channel doping. We have also considered the channel thickness $t_{Si} > 7\,nm$ to eliminate the quantum mechanical effects [Parihar et *al.* (2013)] in the device. The effect of Si channel thickness on the subthreshold current has been shown in Fig.3.6 for t_{Si} = 8 nm, 10 nm, and 12 nm. The increase in the subthreshold current with the channel thickness results from the reduction in gate control over the channel. The variations of subthreshold current as a function of gate-to-source voltages for the two values of projected range (R_p) are shown in Fig. 3.7. The increase in the subthreshold current with R_P is attributed to the decreased threshold voltage due to decreased channel doping at the Si/SiO_2 interface.

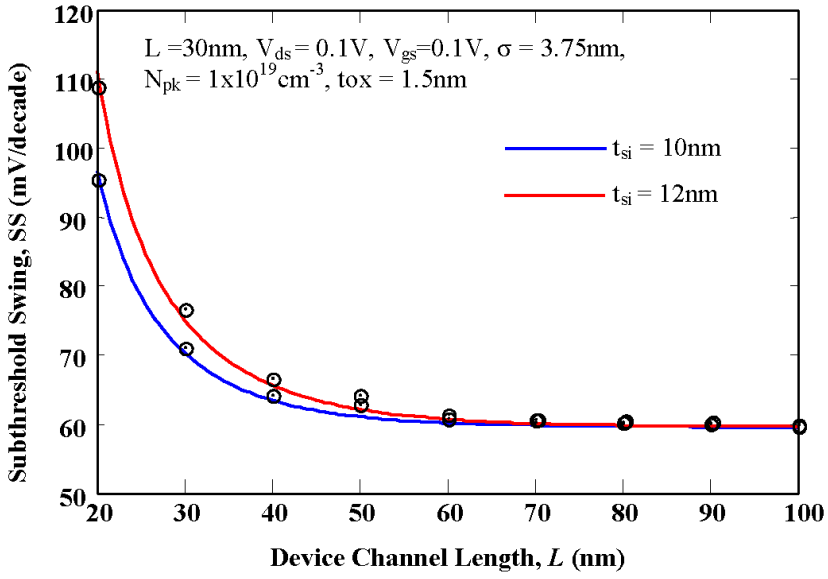

Fig.3.8: Subthreshold swing versus device channel length for different channel thicknesses.

The SS characteristics of the ion-implanted DG-JLFET under study are shown in Fig.3.8 for different channel thickness. It is perceived from the figure that the SS increases significantly with the decrease in the device channel length below 60 nm due to the severe increase in short channel effect. It is further observed from Fig.3.8 that the SS increases with increased channel thickness for a fixed channel length due to the reduction in the gate control on the channel. Thus, the switching performance of the device is degraded with increased channel thickness and decreased channel length.

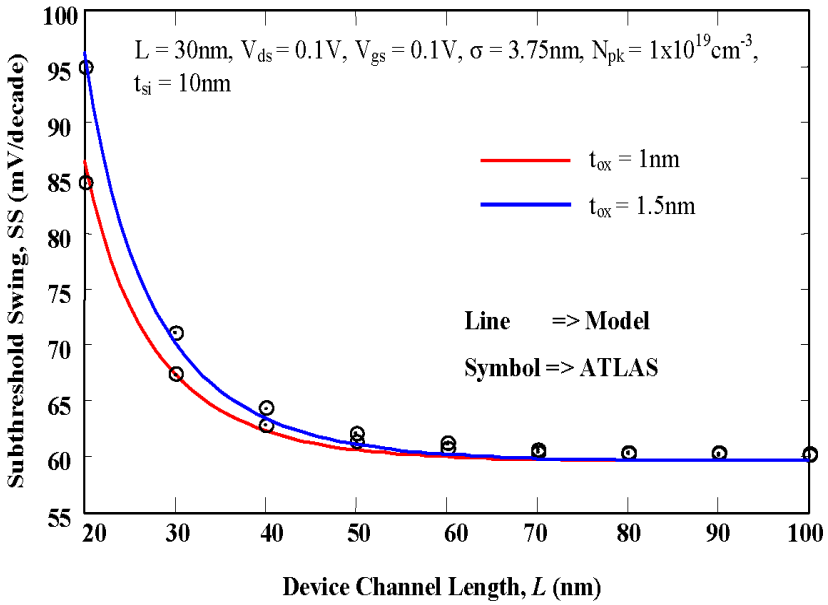

Fig.3.9: Subthreshold swing versus device channel length for different gate oxide thicknesses.

Fig.3.9 shows the variation of SS as a function of device channel length for different gate oxide thicknesses. The SS characteristics are observed to be deteriorated very rapidly with the increased gate oxide thickness for channel lengths below 60nm due to

the reduction in the gate electric fields in the channel.

3.4 Conclusion

This chapter reports two-dimensional modeling of subthreshold current and subthreshold swing of the vertical Gaussian doping channel DG-JLFETs. The actual non-integrable vertical Gaussian doping function has been replaced by a vertical Gaussian-like double-integrable function. It is demonstrated that the subthreshold characteristics of the ion-implanted DG-JLFETs can be controlled not only by the device parameters but also by controlling the channel profile parameters. The subthreshold leakage current is increased with the decreased channel length, increased straggle, increased oxide thickness and increased peak channel concentration of the Gaussian profile. Further, the SS is observed to be deteriorated very rapidly with the increased channel thickness and gate oxide thickness for channel length below 60 nm. The model results have been validated by comparing them with 2D ATLAS ^{TM} TCAD based simulation data.